Advances in Applied Mathematics and Mechanics
Adv. Appl. Math. Mech., Vol. **5**, No. 2, pp. 258-268

DOI: 10.4208/aamm.12-m1238
April 2013

An Empirical Constitutive Correlation for Regular Jugged Discontinuity of Rock Surfaces

Bin Yang[1,2,3,*], Sihao Mo[1], Ping Wu[1] and Chaoqing He[1]

[1] *College of Civil Engineering and Architecture, Guangxi University, Nanning, China*
[2] *Key Laboratory of Disaster Prevention and Structural Safety of Ministry of Education, Nanning, China*
[3] *Guangxi Key Laboratory of Disaster Prevention and Engineering Safety, Nanning, China*

Received 3 April 2012; Accepted (in revised version) 19 November 2012

Available online 8 March 2013

Abstract. This paper presents a physical investigation and mathematical analysis on mechanical behavior of the regular jugged discontinuity. In particular, we focus on the creep property of structural plane with various slope angles under different normal stress through shear creep tests of structural plane under shear stresses. According to the test results, the shear creep property of structural plane was described and the creep velocity and long-term strength of the structural plane during shear creep were also investigated. An empirical formula is finally established to evaluate shear strength of discontinuity and a modified Burger model was proposed to represent the shear deformation property during creep.

AMS subject classifications: 26A33, 65M06, 65M12, 65M60

Key words: Empirical constitutive correlation, discontinuity, mathematical analysis.

1 Introduction

Structural plane is the basic constituent of rock. It is the discontinuous plane which has extremely low or no tensile strength, and it includes all kinds of geological separations, such as, joints, faults, soft interlayers. To some extent, the mechanical property of structural plane controls the mechanical property of engineering rock, determining the scope and types of rock unstable failure. The failure mechanism of a rock mass largely depends on the failure of the structural planes, which is not a rapid or unexpected brittle failure, but one that experiences stress relaxation due to geological time span creep under

*Corresponding author.
Email: yangbin5613@163.com (B. Yang)

long-term loads until final failure. The creep failure of the structural plane is one main reason of engineering rock unstable failure, sometimes even dominating. However, some scholars (Ding et al. [5] and Xu and Yang [14]) argue that the creep property of a structural plane is different from that of the whole rock (practical engineering), without any accelerated creep stage.

The purpose of this research on creep property of the rock mass structural plane is to understand its deformation mechanism, its development and failure, and its time sensitive nature under long-term loads. Researchers all over the world did some work on it. Xu and Xia [13] carried out laboratory creep experiments and proposed a generalized model to explain creep associated with rock mass structural planes in the Three Gorges Project. Ding et al. [5] performed a shear creep test on rigid structural plane of navigation lock area of the Three Gorges Project. This research analyzed the creep behavior of a structural plane under constant loads, and proposed the shear creep equation for structural plane creep. Recent studies have identified the nonlinear rheological property of rock materials. Cao et al. [3] updated the linear coefficients of viscosity in the viscous volume model to nonlinear by analyzing the total stress-strain curve and the rock mass creep curve. Also, he proposed a combined model, which represented the non-decreasing creep property of rock mass. Based on the modified Xiyuan model proposed by Wang and Wang [16], Wang et al. [15] considered that the nonlinear change was accompanied by deformation and hence obtained the stability condition for the modified Xiyuan model through local linearization of the nonlinear creep problem. Xu and Yang [14] proposed a nonlinear viscous element to the triaxial rheological test curve of greenschist and obtained a nonlinear plastic body, which fully represented the accelerated rheologic property of rock mass. There is much scope for the development of more robust models suitable for analysis and design within ground engineering.

In this paper, based on the shear tests and shear creep tests on regular tooth structural planes under different normal stresses, we investigate mechanical properties and mainly, strength characteristics and creep properties of such planes under shearing conditions. Through lots of shear creep laboratory tests of structural plane, it studied the shear creep property of structural plane, and analyzed the deformation property and creep rate property during the creep process. Meanwhile, shear creep constitutive model of the structural plane was proposed, and its applicability was discussed.

2 Physical investigation

The experimental test was carried out with rock biaxial rheological testing machine produced by Changchun Testing Machine Research Institute in China. The machine can apply vertical axial compression (tension) and horizontal axis compression (tension) both simultaneously and separately, and can measure the deformation of both axes and both sides simultaneously. The maximum vertical axial compression load is 500KN; the maximum horizontal axial compression load is 300KN. In this experiment, the maximum axial load is around 50KN. The testing machine is servo controlled, and the compressional stress was applied via a screw rod pressing mechanism. The measuring accuracy of deformation is 0.0001mm, which represented less than 0.01% FS deflection in the tests undertaken. The structural plane is formed between cement mortar tests specimens that have regular jagged surfaces, i.e., the rough surfaces are simplified to one with regular tooth profile of the same slope angle for the purpose of reducing the complexity of the structural planes. In order to avoid the test result difference due to the differences in material strength and deformation of the specimens, each batch of specimens were made of the same materials, the same mix proportion, and the same curing time and were shaped in molds of the same specification.

The specification of a specimen was such that it fitted into a one litre volume $10\times 10\times 10$cm, with a regular jagged structural plane comprising 10 teeth. The tooth profiles have four types of slope angles: 10°, 20°, 30° and 45°. The specimens are made of No. 325 cement, standard sand, and water. The mix proportion of water: cement: sand was 1:2:4. In order to obtain a consistent quality and enhance the compactness, the material was charged and damped layer by layer during casting.

We conducted a compressive strength experiment of one single test specimen to verify the magnitude of the normal stress needed. We can use former relevant experimental data to depict a forecasting curve, and check the curve with a group of test specimens to get the exact normal force. In shearing experiments, the angles of specimens of regular tooth structural planes included 5 types, which were 0°, 10°, 20°, 30°, 45° and each type of specimens were tested under normal stresses of uniaxial compressive strength of respectively 50%, 40%, 30% and 20% ($0.5\sigma_c$, $0.4\sigma_c$, $0.3\sigma_c$ and $0.2\sigma_c$). First, increased normal force to the predetermined values and held them; then increased tangential force with a certain rate until the specimens were damaged.

In order to determine the creep parameters and deformation mechanism of structural plane, shear creep tests of regular jagged structural planes were performed. An incremental step loading technique was adopted to increase the load step by step until the sample was failure. For different slope angles and horizontal stresses, the same vertical stress was applied and kept constant in favor of the experimental data analysis. The vertical stress was chosen as 5% and 15% of the average value of the unconfined uniaxial compression strength of samples with the same structural plane. The horizontal grades of stress were 70%, 80%, 90% and 95% of the limit shear strength under the corresponding axial compression samples with the same structural plane.

3 Theoretical treatments

The relationship between the peak shear strength and slope ratio of discontinuity is shown in Fig. 1 and it can be seen from the figure that there is a very good linear relationship between them. Under a certain normal stress, the shear strength increases as the slope ratio increases. When the slope ratio changes from 10° to 45°, the average in-

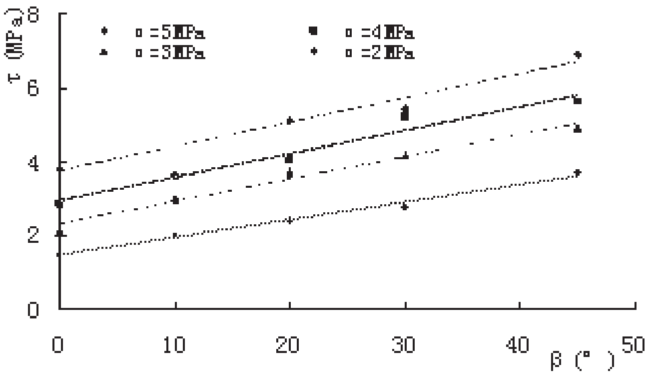

Figure 1: The relationship between peak shear strength and discontinuity angle.

crease of shear strength is around 60%. However, the changing trend and increase of the peak shear strength are different under different normal stresses and slope ratios. As the slope ratio increases, the shear strength of discontinuity increases evidently. The reason is that the dilatancy effect decreases and the shearing through asperities increases, as the slope ratio increases. The slop ratio has a lot of effects on the strength of discontinuity.

Generally, the peak shear strength formula for the discontinuity of rigid rock mass is expressed as:

$$\tau_p = \sigma_n \cdot \tan(\phi_r + i), \tag{3.1}$$

where φ_r is the basic internal friction angle, i is the synthetically slope ratio of discontinuity.

During the shear test, the process of failure includes both the sliding along and shearing through asperities, which vary with the slope ratio. Assuming that the basic internal friction angle is taken unchanged during the shearing process, Eq. (3.1) is modified as follows:

$$\tau_p = \sigma_n \cdot \tan(\phi_r + i) + C_i, \tag{3.2}$$

where φ_r is the basic internal friction angle, corresponding to the internal friction angle of the $0°$ discontinuity. i, which is related to the discontinuity angle β, is the slope ratio which is taken as the sliding on asperities during the shearing process. C_i is cohesion, which is taken as the shearing through asperities. According to Coulomb-Mohr law, the summation of φ_r and i is represented by φ_j, which is the internal friction angle of discontinuity.

It can be seen from the fitting result that the synthetical shear strength parameters of discontinuity C_i and φ_i increase as the slope ratio of the jugged discontinuity increases. Generally, the synthetical shear strength parameters of discontinuity C_i and φ_i remain unchanged for homogeneous materials. However, in this test, almost all the teeth of the sample are sheared after they undergo sliding on asperities to a certain level rather than purely sliding on asperities or shearing through them. The area of cut of the tooth tip changes because of the sliding on asperities, and so do the synthetical shear strength parameters of discontinuity C_i and φ_i. Under the same stress, the sliding on asperities decreases, the shear resistance of the tooth increases, and the area of cut of the tooth tip increases as the slope ratio increases. Therefore, C_i becomes greater. Because of the sliding on asperities, φ_i increases as the slope ratio increases, which matches with the failure mode of the sample observed during the test.

There is a good linear relationship between the synthetical shear strength parameters and the slope ratio. According to the data and curves, an empirical formula similar to Patton formula is proposed as follows:

$$\tau=\sigma_n\cdot\tan(\phi_0+h(\beta))+f(\beta). \tag{3.3}$$

In Eq. (3.3), β is the discontinuity angle and φ_0 is the basic internal friction angle. $h(\beta)$ and $f(\beta)$ are functions of the discontinuity angle, which represents the sliding on asperities and shear through them respectively. According to the linear relationship between the shear strength parameters and the angle of discontinuity, a particular form of Eq. (3.3) can be expressed as follows:

$$\tau=\sigma_n\cdot\tan(\phi_0+K_i\beta)+K_c\beta, \tag{3.4}$$

where K_i is the coefficient of correction for the internal friction angle of discontinuity when loaded, K_c the coefficient of correction for discontinuity cohesion and β taken as a parameter for the roughness of discontinuity. According to the test result, the parameters under shear stress are: $\varphi_0=36^\circ$, $K_i=0.21$, $K_c=0.037$.

The shear creep tests of regular jagged structural planes are under 2 types of vertical stresses: 0.6MPa, 8MPa. Fig. 2 shows the whole shear creep test process of structural planes with different slope angles. From the curve of the whole creep test, it has been discovered that the creep deformation of different angles depends largely on the magnitude of the load level. Under a constant horizontal stress, the shear displacement increases with time. The larger the vertical stress, the larger the horizontal load, which is needed to induce the shear creep failure of the structural plane. The structural planes with different slope angles do not experience the accelerated creep stage during the creep process. When the horizontal stress reaches the last stage, the structural plane slips quickly until failure and the duration is very short.

Usually, the rock mass creep deformation includes four stages: instant deformation, initial creep, steady-state creep. Empirical formula (3.1) can be used to fit the creep curve grading

$$u=u_0+A\cdot\ln t+B\cdot t^n, \tag{3.5}$$

where u_0 is instant deformation; $A\ln t$ is attenuate deformation; Bt^n is the third stage creep; A and B are constants; n is creep index, which represents the nonlinear property of the third stage creep; t is time.

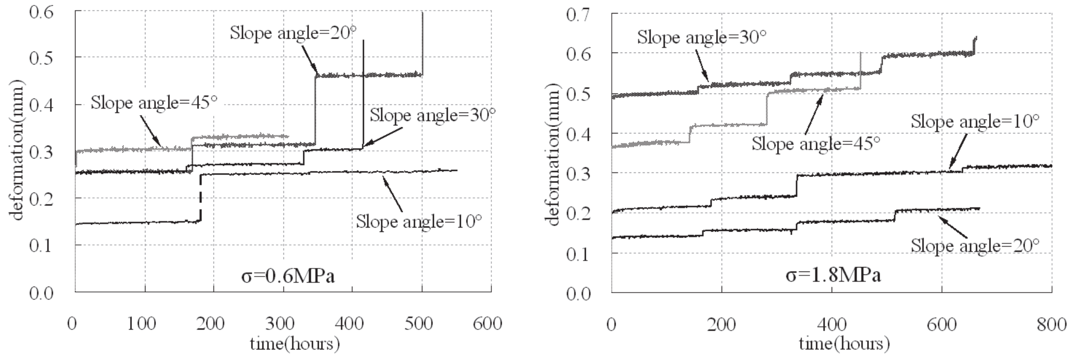

(a) (b)

Figure 2: The curves of shear creep test process of structural planes with different slope angles.

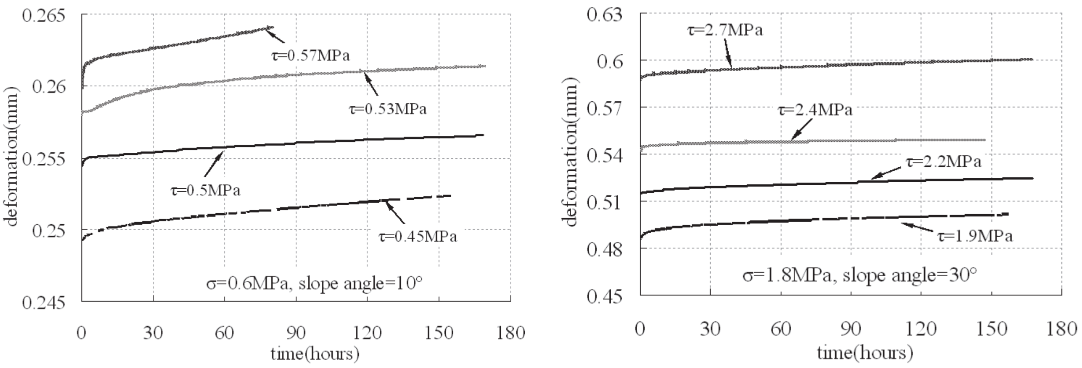

(a) (b)

Figure 3: The grading curves of shear creep of 10° and 30° structural planes.

The individual creep curves for structural planes at each angle were obtained according to the fitting formulas, as shown in Fig. 3 (take 10° and 30° grading curves of the structural planes as examples). By observing the individual creep obtained from every shear creep test for the structural plane specimen, some features of the structural plane shear creep deformation can be concluded as follows.

As soon as the horizontal load is applied, it induces an instant shear deformation and the curve enters the initial creep stage. However, the duration is relatively short. At this stage, the creep velocity changes from a relatively high value to a limited one. The creep velocity of the initial creep decreases quickly. After the initial creep, the state transits towards steady creep with time. This stage is relatively long and the duration mainly depends on the horizontal stress. As time goes by, it transits to the steady-state creep stage, during which the creep velocity decreases with time very slowly; usually, it takes some time from initial creep to stable deformation, and the duration of the process is af-

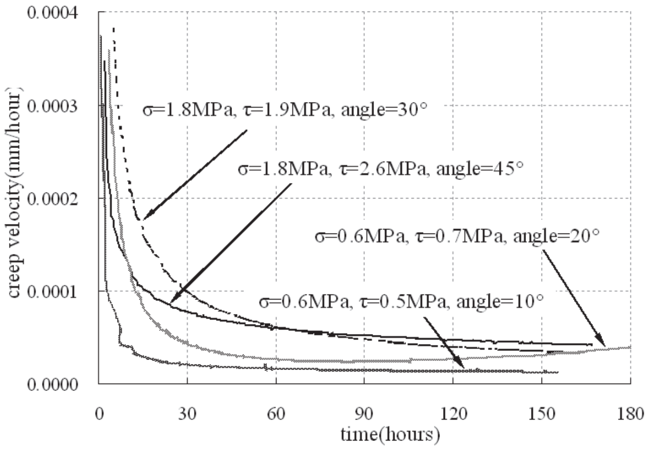

Figure 4: The creep velocity curves of structural planes with different slope angles.

fected by the shear stress. Structural planes with different slope angles do not experience the accelerate creep stage during the process. When the horizontal stress reaches the last stage level, the structural plane slips quickly until failure and the duration is very short.

The creep velocity-time curve can be obtained by calculating the gradient of the creep curve of structural planes with different angles at every moment. Fig. 4 shows the shear creep velocity of some structural planes changing with time under vertical stress. From the graph, it can be seen that the creep velocity curve experiences instant creep, initial creep and steady creep stages. The creep velocity of the initial creep decreases quickly. After a very short period, the structural plane creep transits to the steady-state creep stage, in which the creep velocity is approximately zero but not constant, it changes with time slowly, and the accelerate creep stage is never observed. Under higher shear stress conditions, it takes more time for structural plane creep to transit from initial creep stage to steady-state creep stage. In the steady-state creep stage, the amplitude of variation is small enough for it to be considered as a steady-state creep. As shown in Fig. 4, the creep velocity curves of structural planes with different slope angles have similar characteristics, after they have stabilized, they have close creep velocities.

From the relation curve of creep velocity and time, it can be observed that the creep velocity has an initial creep velocity at the test beginning stage, as time goes by, the creep velocity decreases gradually and tends to stabilize. Through the comparative analysis of curves, it is found that formula (3.2) can be used to describe the relation curve of creep velocity and time (Fig. 5)

$$v=v_0+\frac{A}{t^n}, \tag{3.6}$$

where v is creep velocity; v_0 is initial creep velocity; t is time; A and n are constants.

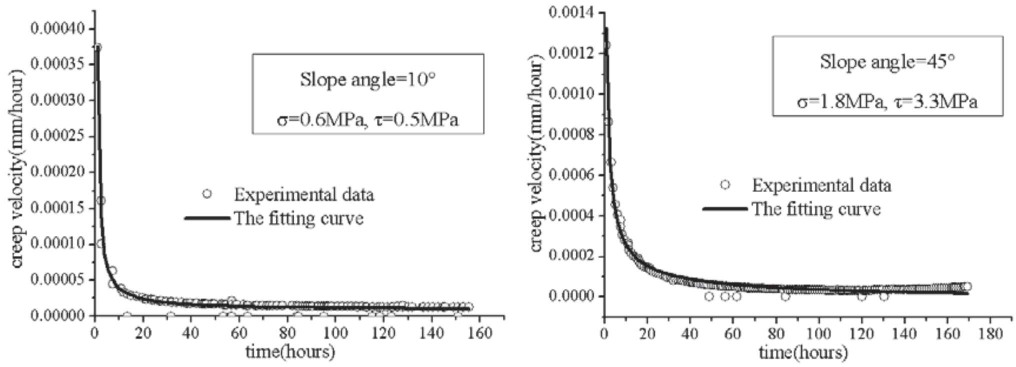

Figure 5: The fitting curves of creep velocity of structural planes.

4 Mathematical analysis

Creep theoretical models have many basic forms, as to the rock and soil mass material, the test curves must be analyzed briefly before the creep theoretical model is determined. Based on the test results, we proposes a nonlinear viscous element according to the features of the structural plane creep curves, and makes some modifications about Burger model for a better representation of the structural plane creep curve. Fig. 6 shows the modified Burger model, which can be used to describe the structural plane shear creep curve. The modified Burger model is used to fit the shear creep curves, and it can describe the viscoelastic creep properties.

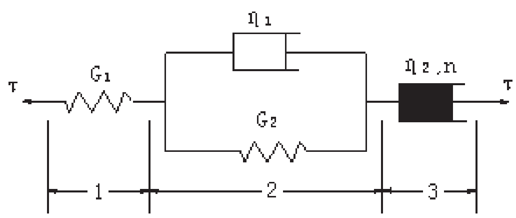

Figure 6: Modified Burger model.

According to the relation in the figure, the model satisfies the following condition, since it is combination in series:

$$\tau=\tau_1=\tau_2=\tau_3, \tag{4.1a}$$
$$\gamma=\gamma_1+\gamma_2+\gamma_3, \tag{4.1b}$$
$$\tau_1=G_1\cdot\gamma_1, \tag{4.1c}$$
$$\tau_2=\eta_1\cdot\dot{\gamma}_2+G_2\cdot\gamma_2, \tag{4.1d}$$
$$\tau_3=\eta_2\cdot\dot{\gamma}_3/(nt^{n-1}), \tag{4.1e}$$

where G_1, G_2 are shear modulus, η_1, η_2 are coefficients of viscosity, n is rheological index.

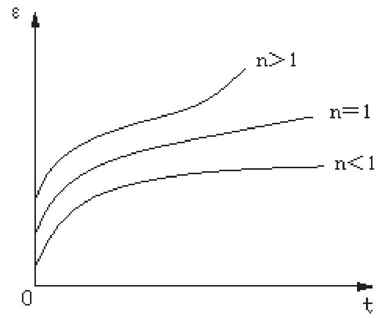

Figure 7: Creep curves of modified Burger model.

The constitutive relation for the rheological mode can be deduced from formula (3.3)-(4.1a), as follows:

$$\ddot{\gamma}+\frac{G_2}{\eta_1}\dot{\gamma}=\frac{\ddot{\tau}}{G_1}+\left(\frac{1}{\eta_1}+\frac{G_2}{G_1\cdot\eta_1}+\frac{n\cdot t^{n-1}}{\eta_2}\right)\cdot\dot{\tau}+\left[\frac{G_2\cdot n\cdot t^{n-1}}{\eta_2\cdot\eta_1}+\frac{n\cdot(n-1)\cdot t^{n-2}}{\eta_2}\right]\cdot\tau. \tag{4.2}$$

If the initial conditions are: $t=0$, $\gamma=\tau_0/G_1$ and $\tau=\tau_0$, the creep function for the model can be deduced from the rheological constitutive relation as follows:

$$\gamma=\tau_0\left\{\frac{1}{G_1}+\frac{1}{G_2}\left[1-\exp\left(-\frac{G_2}{\eta_2}t\right)\right]+\frac{t^n}{\eta_1}\right\}. \tag{4.3}$$

Based on the creep function of the new model, and compare it with the creep function of the Burger model, a rheological index n is included in the mathematical expression in the modified Burger model creep function that represents the nonlinear relation between creep deformation and time, as shown in Fig. 7.

It can be seen from this experiment and the curve fitting results (Fig. 8, take the curves of 20° and 30° structural planes as examples) that, the modified Burger model matches well with the structural plane shear creep test results. The modified Burger model represents the creep process of the structural planes in detail. The model represents that the structural plane creep velocity decreases with time. The modified Burger model is of a simpler form, and it is not complicated for determining the parameters, which have clear meanings. It is convenient to carry out curve fitting analysis on the structural plane creep property and hence practical.

5 Conclusions

The shear tests and shear creep tests are carried out on the regular jugged discontinuity with different angles and under different stresses in this study. During the shearing process, both the sliding on asperities and shearing are included in the failure mode of discontinuity. According to the data and curves obtained, an empirical equation is proposed with a form similar to the Patton Equation. The shear creep failure of a structural

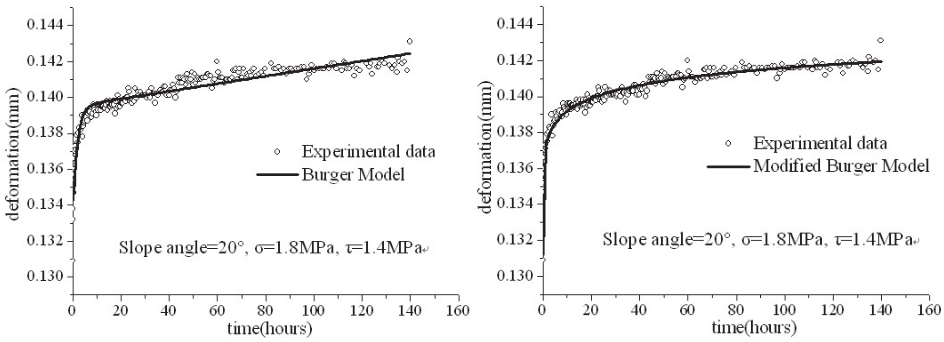

(a)

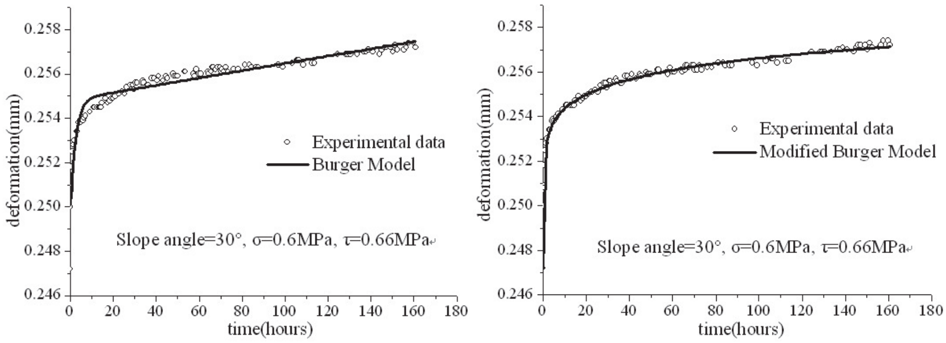

(b)

Figure 8: The test curves fitting graph of the modified Burger model and Burger model.

plane exhibits an obvious instant deformation property, which is very important for engineering rocks with well developed structural planes. The structural plane creep velocity starts from an initial creep velocity. In the process of test, the creep velocity decreases in the form of index decreasing and finally tends to stabilize. The modified Burger model matches with the structural plane shear creep test results very well.

The structural plane specimens are artificial regular jagged structural planes, the more comprehensive study should changes from regular jagged structural planes to natural structural planes. And the creep constitutive model of structural planes in this study do not introduce any parameters which represent structural plane properties, and this worth to be studied further. Through the creep test of structural plane, hopefully a more reasonable method can be found to evaluate the long-term strength of structural plane, thus can instruct the practical engineering application.

Acknowledgments

This work was supported by National Natural Science Foundation of China (51168005, 51268003), Key Project of Guangxi Scientific Research and Technological Development Plan (10124006-10), Key Project of Guangxi Science and Technology Lab Center (LGZX201107), Natural Science Foundation of Guangxi (2012GXNSFAA053205), and Foundation Project of Guangxi Key Laboratory of Disaster Prevention and Engineering Safety (2009TMZR004, 2012ZDX08).

References

[1] G. N. BOUKHAROV AND M. W. CHANDA, *The three processes of brittle crystalline rock creep*, Int. J. Rock Mech. Mining Sci., 32(4) (1995), pp. 325–335.

[2] R. K. BOWDEN, Time-Dependent Behavior of Joints in Shale, MA.Sc. Thesis, University of Toronto, Ontario, 1984.

[3] S. G. CAO, B. JIN AND P. LI, *Rheologic constitutive relationship of rocks and a modifical model*, Chinese J. Rock Mech. Eng., 21(5) (2002), pp. 632–634.

[4] J. H. CURRAN AND A. M. CRAWFORD, *A comparative study of creep in rock and its discontinuities*, Proc. of the 21st U.S. National Rock Mechanics Symposium, Rolla, Missouri, 596–603, 1980.

[5] X. L. DING, J. LIU AND X. Z. LIU, *Experimental study on creep behaviors of hard structural plane in TGP s permanent lock regions*, Journal of Yangtze River Scientific Research Institute, 8 (2000), pp. 30–33.

[6] G. FABRE AND F. PELLET, *Creep and time-dependent damage in argillaceous rocks*, Int. J. Rock Mech. Mining Sci., 43(6) (2006), pp. 950–960.

[7] Y. FUJII AND T. KIYAMA, *Circumferential strain behavior during creep tests of brittle rocks*, Int. J. Rock Mech. Mining Sci., 6 (1999), pp. 323–337.

[8] L. JING, E. NORDLUND AND O. STEPHANSSON, *A 3D constitutive model for rock joints with anisotropic friction and stress dependency in shear stiffness*, Int. J. Rock Mech. Mining Sci. Geomechanics Abstracts, 31(2) (1994), pp. 173–178.

[9] Y. S. LI AND C. C. XIA, *Time-dependent tests on intact rocks in uniaxial compression*, Int. J. Rock Mech. Mining Sci., 37(3) (2000), pp. 467–475.

[10] E. MARANINI AND M. BRIGNOLI, *Creep behavior of a weak rock: experimental characterization*, Int. J. Rock Mech. Mining Sci., 36(1) (1999), pp. 127–138.

[11] S. OKUBO, Y. NISHIMATSU AND K. FUKUI, *Complete creep curves under uniaxial compression*, Int. J. Rock Mech. Mining Sci. Geomechanics Abstracts, 28(1) (1991), pp. 77–82.

[12] D. STERPI AND G. GIODA, *Visco-plastic behavior around advancing tunnels in squeezing rock*, Rock Mech. Rock Eng., 23(3) (2007), pp. 292–299.

[13] P. XU AND X. L. XIA, *A study on the creep model of rock mass discontinuity of the three gorges project*, Journal of Yangtze River Scientific Research Institute, 3 (1992), pp. 42–45.

[14] W. Y. XU AND S. Q. YANG, *Test study on shear rheological behavior of jointed rock mass and the model investigations*, Chinese Journal of Rock Mechanics and Engineering, 24(Supp.2) (2005), pp. 5536–5542.

[15] L. G. WANG, F. HE, X. H. LIU AND Y. J. YU, *Non-linear creep model and stability analysis of rock*, Chinese Journal of Rock Mechanics and Engineering, 23(10) (2004), pp. 1640–1642.

[16] Y. J. WANG AND L. G. WANG, *Rheology instability theory of submerged rock body*, China's Mining Industry, 3(1) (1994), pp. 36–40.

[17] M. L. ZHU, Z. D. ZHU AND Z. J. LI, *Preliminary study of non-stationary shear rheological model of wall rock of long, large and deep-buried tunnel*, Chinese Journal of Rock Mechanics and Engineering, 27(7) (2008), pp. 1436–1441.